JAAS

Accepted Manuscript

This is an *Accepted Manuscript*, which has been through the Royal Society of Chemistry peer review process and has been accepted for publication.

Accepted Manuscripts are published online shortly after acceptance, before technical editing, formatting and proof reading. Using this free service, authors can make their results available to the community, in citable form, before we publish the edited article. We will replace this *Accepted Manuscript* with the edited and formatted *Advance Article* as soon as it is available.

You can find more information about *Accepted Manuscripts* in the Information for Authors.

Please note that technical editing may introduce minor changes to the text and/or graphics, which may alter content. The journal's standard Terms & Conditions and the Ethical guidelines still apply. In no event shall the Royal Society of Chemistry be held responsible for any errors or omissions in this *Accepted Manuscript* or any consequences arising from the use of any information it contains.

ROYAL SOCIETY OF CHEMISTRY

www.rsc.org/jaas

Graphical Abstract

High resolution sector field ICP-MS (SF-ICP-MS) is used to explore the mechanisms and limitations of the interference standard method (IFS).

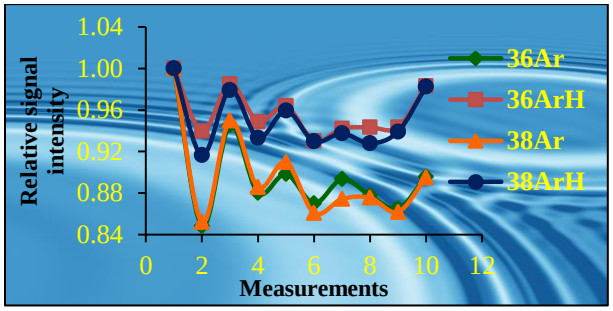

Interference standard method: evidence of principle, potentialities and limitations

Renata S. Amais,[a] Joaquim A. Nóbrega[a*] and George L. Donati[b]

[a]Group of Applied Instrumental Analysis, Department of Chemistry,

Federal University of São Carlos, São Carlos, SP, Brazil

[b] Department of Chemistry, Wake Forest University, Winston-Salem, North Carolina,

USA

This study was presented at the 2014 Winter Conference on Plasma Spectrochemistry

* Corresponding author. Tel.: +55 16 33518058. Fax: +55 16 33518350.

E-mail: djan@terra.com

Abstract

The interference standard method (IFS) is a calibration approach recently proposed to overcome polyatomic interferences in quadrupole-based inductively coupled mass spectrometry (ICP-QMS). Based on the hypothesis that interfering ions and IFS species such as $^{36}Ar^+$, $^{36}ArH^+$ and $^{38}Ar^+$ present similar behaviors in the plasma, the IFS method has successfully been applied in several analytical procedures. In this work, analyte, interfering ions and IFS species are monitored by high-resolution double focused sector field inductively coupled plasma mass spectrometry (HR-SF-ICP-MS) to achieve a better understanding of the IFS method mechanisms. The relationship between accuracy and signal variations for interfering and IFS species is explored. Critical cases of polyatomic interferences in elemental determination by quadrupole-based ICP-MS instruments, such as the ones observed for $^{39}K^+$, $^{75}As^+$, $^{28}Si^+$ and $^{32}S^+$, are evaluated. The limitations of the IFS method and the conditions in which it can be most effective are discussed. This is a simple and efficient method that could be extended to other analytical techniques provided that interfering and IFS species present similar signal behaviors.

Key words: IFS method, ICP-MS, polyatomic interfering ions, accuracy, high resolution.

Introduction

Inductively coupled plasma mass spectrometry (ICP-MS) has been recognized as one of the most powerful analytical techniques available for trace element determinations, with important applications in several fields, such as environmental, geochemistry, agriculture, semiconductors, fuel analysis and medical/clinical.[1] Nowadays, ICP-MS applications have been expanded by using hyphenated techniques[2] such as those using chromatography[3], laser ablation[4] and separation flow systems[5]. In spite of being increasingly used in routine analysis, this technique still presents some challenges; especially for quadrupole-based instruments (ICP-QMS). Polyatomic interfering ions are the major factor contributing to relatively poor sensitivities and accuracies in certain ICP-QMS determinations. Argon-, nitrogen- and oxygen-containing species are the most critical cases of spectral interferences since they are produced from naturally occurring molecules in the plasma: the plasma gas itself or atmosphere gases diffusing into the plasma.[6] In addition, these species present low mass/charge ratios (m/z below 82), which overlap with several important low m/z elements.[7,8] For example, $^{38}ArH^+$, $^{40}Ar^{16}O^+$, $^{14}N_2^+$, and $^{16}O_2^+$ are directly related to $^{39}K^+$, $^{56}Fe^+$, $^{28}Si^+$ and $^{32}S^+$ high background signals.[9]

Collision-reaction cells and interfaces are instrumental alternatives that have been successfully used in routine and research applications to minimize spectral interferences in ICP-MS determinations.[10-12] These are commercially available technologies that employ instrumental devices (cells or special cones) and additional gases (*e.g.* He, H_2, O_2 and CH_4), which interact with analytes and interfering ions to minimize spectral interferences by curbing polyatomic ion formation and/or reducing the interfering ion kinetic energy.[10-12] Another successful alternative that is related to significant improvements of resolving power is the use of high-resolution ICP-MS instruments, such as double focusing mass analyzers, which allowed the determination of

several difficult elements even in complex matrices.[13] However, the relatively high cost of high-resolution instruments still prevents a wider use of this technology. On the other hand, cool plasma, mathematical equations and sample preparation are some less expensive alternatives commonly used to overcome these same limitations.[6,12-15] In this case, although efficient, these strategies are applicable to few particular cases.[15]

More recently, Donati *et al.*[16] proposed the interference standard (IFS) method as an alternative approach to improve accuracy in ICP-QMS determinations. Because the signal intensity of an interfering ion is usually much higher than the analyte's, a minimal variation in the interfering ion signal can compromise accuracy in typically low-resolution quadrupole-based instruments. The IFS method is based on the hypothesis that interfering ions have the same behavior as the IFS species (i.e. ions naturally present in the plasma such as $^{36}Ar^{+}$, $^{36}ArH^{+}$ and $^{38}Ar^{+}$). Similarly to an internal standard (IS) method, the ratio between the non-resolved total analytical signal (interfering ion plus analyte) and the IFS signal is used for calibration. Thus, if IFS and interfering species have similar behaviors, one can minimize the interfering ion contribution to variations in the total analytical signal.[16] The main difference between IFS and IS is that while the latter uses species with behaviors similar to the analyte, the former uses the ones behaving like the interfering species. The main advantages of the IFS method are its simplicity and the fact that it requires no instrumental modifications or additional gases.[16,17]

Analytical procedures using the IFS method have been applied to As, K, P and Si determinations in standard reference materials (SRM) of apple leaves, water, bovine liver and typical diet[16]; to Fe, Mn and S determinations in grains and meat;[18] and to S determination in biodiesel and lubricant oil using microemulsion preparation for direct analysis.[19] This method was also successfully applied to improve accuracy in P and S determinations in fuels by

monitoring oxide and hydroxide species, i.e. PO^+ and SOH^+.[20] Although efficient at minimizing spectral interferences, the mechanisms involved in the IFS method and its main limitations are still little understood. In this work, we explore the relationship between accuracy and signal variations for interfering and IFS species. Analyte, IFS and interfering species are monitored using a high-resolution sector field ICP-MS (SF-ICP-MS) instrument, and additional evidence of the IFS method's principle, as well as some of its main limitations are presented.

Experimental

SF-ICP-MS measurements

A high-resolution sector field double focused inductively coupled mass spectrometer (HR-SF-ICP-MS) (Element XR, Thermo Scientific, Waltham, MA, USA) was used in all measurements. The sample introduction system is composed of a concentric nebulizer and high stability chamber, which combines a cyclonic and a double-pass spray chamber. Table 1 presents the instrumental conditions used in this work. The mass ranges and setting times of each species monitored are shown in Table 2. All measurements were carried out by monitoring 3 runs and 15 passes.

Analytical solutions

All solutions were prepared using distilled-deionized water (18.2 MΩ cm resistivity) produced by a Milli-Q Element system (Millipore, Billerica, MA, USA). High purity grade nitric acid and hydrochloric acid (Optima, Fisher Scientific, Fairlawn, NJ, USA), as well as standard reference solutions of As (SRM 3103a), Fe (SRM 3126a), K (SRM 3141a), S (SRM 3154) and Si (SRM 3150), and a standard reference material of trace elements in water (SRM 1643e) were

used in this work. All standard reference solutions and standard reference material are from the National Institute of Standards and Technology (NIST, Gaithersburg, MD, USA). Tap water collected immediately before analysis was used in addition and recovery experiments.

Results and discussion

Behaviors of interfering ions and IFS species

Potassium

Accuracy in $^{39}K^+$ determinations by ICP-QMS is severely compromised by spectral interference caused by the $^{38}ArH^+$ ion. While monitoring both analytical (I_A, $^{39}K^+$) and interfering (I_I, $^{38}ArH^+$) signals of a 5 µg L^{-1} K solution by high-resolution SF-ICP-MS, it was observed that I_I is 7.5-fold higher than I_A. Thus, according to data previously published[16], a variation of 5 % in the $^{38}ArH^+$ signal, for example, would represent a 137.5 % recovery for K while using a quadrupole-based instrument. Such signal and recovery discrepancy would be expected to be even larger in real ICP-QMS conditions since ion transmission in the present high resolution instrument is only approximately 2% of the one observed in low resolution measurements.[13] Considering that an IFS species has the same behavior as the interfering ion, the interfering signal variation would be minimized by using the analytical/IFS signal ratio in the calibration, which would improve accuracy.

Figure 1 shows signal profiles of the polyatomic interfering ion $^{38}ArH^+$ and the IFS species, $^{36}Ar^+$, $^{36}ArH^+$ and $^{38}Ar^+$, while alternatingly introducing K standard solutions diluted in HNO_3 1% (v/v) (blank, 1, 5, 20 and 50 µg L^{-1}) and trace elements in water (SRM 1643e) diluted in HNO_3 1% (v/v) (for a final K concentration of 1, 5, 20 and 50 µg L^{-1}) into a SF-ICP-MS

instrument. The relative signal intensities were normalized to fit the same scale (*i.e.* all signals of a certain species were divided by its highest signal). As it can be seen, in this case, interfering and IFS species present exactly the same behavior in the plasma. It is possible that the different signal fluctuations observed for the blank and the sample replicates are a result of small variations in parameters such as temperature, number of ions extracted, local electron density and different chemical processes. As it would be expected, the $^{36}ArH^{+}$ ion resembles the interfering ion more closely because it is composed of the same elements. Thus, both interfering and IFS species experience the same signal fluctuations. Although in a slightly different scale, the other IFS probes also present similar signal profiles to the interfering ion, and can be successfully used to improve accuracy in K determinations by ICP-QMS.[16] This is an obvious application of the IFS method since one would expect the same behavior for species composed of the same elements. The chemical interactions and reactions involving argon species in the plasma would then have the same effect on both interfering and IFS species, which would result in similar signal profiles.

Arsenic

Although the main interfering ion in arsenic determinations also contains argon ($^{40}Ar^{35}Cl^{+}$), this is a different case from K because the polyatomic species is only formed if the sample contains Cl atoms in its composition. To check the signal profiles of $^{40}Ar^{35}Cl^{+}$ and the IFS species, reference standard solutions containing As at 1, 5, 20 and 50 µg L^{-1} in HCl 1 % v/v, and SRM 1643e diluted in HCl (1 % v/v) with the same As concentrations as the reference solutions were analyzed. The IFS probes along with $^{75}As^{+}$ and $^{40}Ar^{35}Cl^{+}$ were monitored by HR-SF-ICP-MS. In this example, variations in the interfering ion signal are only caused by variation

in $^{40}Ar^{35}Cl^+$ formation in the plasma for different samples since Cl concentrations are the same for both solutions. As it can be seen in Figure 2, interfering ion and IFS species present slightly different signal profiles. To simulate the analytical signal that would be obtained with a quadrupole-based instrument, signal intensities of $^{40}Ar^{35}Cl^+$ and $^{75}As^+$ were summed and the comparison between standard reference solutions and samples is presented in Figure 3. Despite small differences in signal profiles (Fig. 2), using the ratio between total analytical signal (analyte plus interfering ion)/IFS signal can improve accuracy (Fig. 3). Considering that the more similar the signal profiles between interfering and IFS species the better the signal correction, $^{36}Ar^+$ and $^{38}Ar^+$ should be more adequate as IFS probes in As determinations as demonstrated in Figs. 2 and 3, and in a previous work.[16]

Silicon and sulfur

Because of the presence of nitrogen, oxygen and carbon dioxide in the atmosphere,[21] polyatomic species generated from these compounds can significantly influence background signals in ICP-MS. Ions such as $^{14}N_2^+$, $^{12}C^{16}O^+$ and $^{16}O_2^+$, for example, compromise accuracy in $^{28}Si^+$ and $^{32}S^+$ determinations. Although these species present no Ar atom, the IFS method with $^{36}Ar^+$, $^{36}ArH^+$ and $^{38}Ar^+$ has successfully been applied in Si and S determinations.[16-20] Figure 4 presents the signal profiles for the IFS species $^{36}Ar^+$, $^{36}ArH^+$ and $^{38}Ar^+$, and $^{14}N_2^+$ plus $^{12}C^{16}O^+$ (as it would be observed at m/z 28 in a low resolution instrument) while alternatively introducing HNO_3 1% v/v and tap water 100-fold diluted in HNO_3 1% v/v. As it can be observed, these species' behaviors in the plasma are similar, which is an indication that they experiment the same effects from fluctuations in physical and/or chemical conditions during signal collection. Similar results are presented in Figure 5 while alternatingly introducing HNO_3 1% v/v and tap water and

monitoring $^{36}Ar^+$, $^{36}ArH^+$, $^{38}Ar^+$ and the main polyatomic interfering ion in S determinations, *i.e.* $^{16}O_2^+$. The reasons to such similar behavior for different species are difficult to explain, especially considering their participation in several complex interactions in the plasma. However, the practical aspects of taking advantage of their similar behavior to correct analytical signal fluctuations and improve accuracy may be useful in different analytical procedures.[16-20] It is possible that the behaviors observed in Figures 4 and 5 would be similar even in different plasma conditions, such as lower applied radio-frequency power and higher nebulization gas flow rates. Evidence for such hypothesis can be found in a previously published study describing the application of the IFS method in S and P determinations by their oxide ions detections.[20]

As it will be discussed in the next section, accuracy improvements are dependent on how similar signal intensity variations occur for interfering and IFS species. In high-resolution determinations at m/z 32, for example, the maximum signal intensity difference between standard solution and sample for the $^{16}O_2^+$ ion was 1.5 x 10^5 cps. For the $^{36}Ar^+$ IFS probe, the difference was 1.7 x 10^5 cps, which is closer to the interfering ion when compared to the other IFS species, *i.e.* 2.1 x 10^3 and 7.7 x 10^4 cps for $^{36}ArH^+$ and $^{38}Ar^+$, respectively. These results corroborate what was observed in a previous work,[19] in which the most accurate results in S determinations by a quadrupole-based instrument were obtained by using the $^{36}Ar^+$ IFS probe.

IFS efficiency and limitations

As proposed by Donati *et al.*[16], recoveries in quadrupole-based instruments for analytes severely affected by polyatomic interfering ions are dependent on how large the interfering ion signal (I_I) is compared to the analyte's signal (I_A), and on how the interfering ion signal varies from the standard reference solution to the sample (I_IV_I, where V_I is the variation in the

interfering ion signal in %). Consider, for example, a blank solution that produces a background signal at the analyte's m/z equals to I_I. While monitoring a standard reference solution, the total analytical signal (I_T) will be equal to $I_A + I_I$. For a sample with the same concentration as the standard reference solution, the total analytical signal will be $I_A + (I_I + I_I V_I)$. In this case, one considers some variation in the interfering ion signal from the standard to the sample, $I_I V_I$. The net signal ($I_T - I_I$) in each case will then be: blank = 0; standard = I_A; and sample = $I_A + I_I V_I$. Thus, recovery (R) will be calculated as follows:

$$R\ (\%) = \frac{Sample}{Standard} * 100$$

$$R\ (\%) = \left(\frac{I_A + I_I V_I}{I_A}\right) * 100$$

$$R\ (\%) = \left(1 + \frac{I_I V_I}{I_A}\right) * 100 \qquad \textbf{(1)}$$

From Eqn. 1,[16] it can be inferred that if the analyte signal (I_A) is considerably higher than the interfering signal (I_I), variations in the latter will have little influence on accuracy. On the other hand, small variations in a significantly higher interfering signal will result in poor accuracy. These effects can be observed experimentally in Tables 3 and 4. When I_I/I_A was 7.5, a variation of - 3.1 % in I_I resulted in a recovery of 61.3 %. For I_I/I_A = 0.8, a variation of 4.6 % in I_I resulted in a 105 % recovery. It is important to note that differences between mathematically calculated and experimentally determined values in Table 3 could be attributed to parameters such as fluctuations in the analyte signal (I_A) or other parameters that were not considered in Eqn.1. Larger discrepancies for lower analyte concentrations indicate that fluctuations in I_A may be the most probable source of error.

Considering the IFS method's principle that accuracy improvements are possible if IFS and interfering species present similar behaviors in the plasma, and that variations in the interfering signal may be minimized by calibrations using the ratio analytical ($I_T = I_A + I_I$)/IFS signal, one can propose the inclusion of the IFS signal in Eq. (1). In this case, total analytical signals (I_T) for blank, standard reference and sample solutions would be $\frac{I_I}{I_{IFS}}$; $\frac{I_A+I_I}{I_{IFS}}$; and $\frac{I_A+(I_I+I_IV_I)}{(I_{IFS}+I_{IFS}V_{IFS})}$, respectively. Here, variations in the interfering (I_IV_I) and the IFS ($I_{IFS}V_{IFS}$) signals from the standard to the sample are considered. Thus, the net signals (I_T - $\frac{I_I}{I_{IFS}}$) will be: blank = 0; standard = $\frac{I_A}{I_{IFS}}$; and sample = $\frac{I_A+I_I(V_I-V_{IFS})}{I_{IFS}(1+V_{IFS})}$. The recovery (R) will then be:

$$R\ (\%) = \left(\frac{\frac{I_A + I_I(V_I - V_{IFS})}{I_{IFS}(1 + V_{IFS})}}{\frac{I_A}{I_{IFS}}} \right) * 100$$

$$R\ (\%) = \left(\frac{I_A + I_I(V_I - V_{IFS})}{I_A(1 + V_{IFS})} \right) * 100$$

$$R\ (\%) = \left(\frac{1}{(1+V_{IFS})} + \frac{I_I}{I_A} * \frac{(V_I - V_{IFS})}{(1+V_{IFS})} \right) * 100 \qquad \textbf{(2)}$$

Some interesting observations can be made based on Eqn. 2. The magnitude of the IFS signal (I_{IFS}) has no effect on recovery; however, its fluctuation (V_{IFS}) is important since it is part of all equation terms. Because interfering and analytical signals are indistinguishable in a quadrupole-based instrument, and the IFS signal divides the combination of both (total analytical signal, I_T), variations in the IFS signal can affect the results. For example, assuming that no other

parameters affect accuracy in ICP-QMS determinations, if $I_I/I_A = 2$, and $V_I = V_{IFS} = 1$ %, R will be 99 %. On the other hand, recovery will go down to 91.7 % if the same conditions remain, but $V_I = V_{IFS} = 9$ %. If $V_I \neq V_{IFS}$ this effect becomes even more significant: if the same conditions remain, but $V_I = 1$ % and $V_{IFS} = 9$ %, R will be 77.1 %.

As demonstrated in the previous section, the main requisite in the IFS method is that interfering and IFS species have similar behaviors in the plasma. Thus, the method will be more effective when $V_I = V_{IFS}$. From Eqn. 2, one can observe IFS's direct effect on interfering ion fluctuations responsible for poor accuracy. Variations in the interfering signal (V_I) are minimized by similar variations in the IFS signal (V_I - V_{IFS}). In this case, the interfering signal can be several times higher than the analyte signal (I_I/I_A) without compromising accuracy. Alternatively, small differences between V_I and V_{IFS} are less important to accuracy when I_I/I_A is small, but become significant for high values of I_I/I_A. For example, if no other parameters are considered, R will be 101 % for $I_I/I_A = 2$, $V_I = 2$ % and $V_{IFS} = 1$ %. For the same conditions with $I_I/I_A = 200$, R would be 297 %. To demonstrate some of these effects, experimental recoveries for $^{38}K^+$ determinations in SRM 1643e at different concentrations are compared to expected values according to Eqn.2 (Table 3). All species were monitored by HR-SF-ICP-MS, but to simulate quadrupole-based low resolution conditions, $^{39}K^+$ and $^{38}ArH^+$ signals were summed and used as the total analytical signal. It is interesting to note that the IFS species presenting the most similar behavior to the interfering species (Fig. 1) is the most effective one at improving accuracy. This is especially true at lower concentrations where using the IFS method is more critical. Recoveries of 61.3 and 102.8 % are obtained for K determinations at m/z 39 for low resolution ICP-MS determinations without applying the IFS method and using the $^{36}ArH^+$ species as IFS probe, respectively (Table 3).

Some of IFS method's limitations can also be inferred from Eqn. 2. For example, if I_I/I_A is large, the difference in signal variations for interfering and IFS species (V_I - V_{IFS}) must be small for the method to be efficient. On the other hand, if V_I - V_{IFS} is large, I_I/I_A must be small to achieve adequate recoveries. In addition, large variations in the IFS signal can also compromise accuracy, even if $V_I = V_{IFS}$, as it can be observed by evaluating the effects of the second term in Eqn. 2. For example, if $V_{IFS} = V_I = 20$ %, R will be 80 %. In that case, if I_I/I_A is small, the IFS method may be discarded. However, deciding whether or not to use the IFS method becomes easy since both analytical and IFS species are monitored during the analysis. Thus, one can choose either the analytical signal itself or the analytical/IFS signal ratio while building the calibration curves.

Conclusions

In this work, some additional evidence of the IFS method principle was presented. Argon species naturally occurring in the plasma present similar signal profiles to interfering polyatomic species, and may experience similar effects from physical-chemical changes such as energy available and gas composition. However, fully understanding the mechanisms responsible for such similarities and for the IFS method efficiency is difficult due to the plasma complexity. Particularly intriguing is the behavior similarities observed for interfering and IFS species composed of different elements. It is possible, in this case, that signal profiles would become more or less similar according to different plasma conditions, and that there would be an ideal set of parameters in which a certain IFS probe would be more efficient. Such hypothesis, if confirmed, would allow a better control of the IFS mechanism and even the development of

procedures tailored to specific combinations of interfering ions, IFS species and plasma parameters. However, more studies are required to check this hypothesis.

Results presented here indicate that IFS's main principle (*i.e.* interfering ions and IFS probes have similar behaviors in the plasma) is correct and that using the analytical/IFS signal ratio for calibration can improve accuracy in K, As, Si and S determinations by quadrupole-based ICP-MS. The results also provide evidence of the method's limitations and the conditions in which it can be most effective at minimizing spectral interferences and improving accuracy. The more similar the signal variations between IFS (V_{IFS}) and interfering species (V_I) the better the accuracy. Best performances would then be observed when I_I/I_A is small or when $V_I \approx V_{IFS}$. On the other hand, large variations in the IFS signal may also compromise accuracy. In this case, however, the IFS species chosen may not be adequate and a new one should be evaluated. Finally, one can infer that the IFS method may be applicable to other analytical techniques provided the interfering species are known and an IFS species is available.

Acknowledgments

The authors are thankful for the grants 2006/59083-9, 2010/17387-7, 2012/00920-0 and 2010/50238-5 São Paulo Research Foundation (FAPESP) and the Conselho Nacional de Desenvolvimento Científico e Tecnológico (CNPq). The support from the National Institute of Standards and Technology (NIST – Charleston, SC, USA), mainly provided by Dr. Stephen E. Long and Dr. Steven J. Christopher, and the Hollings Marine Laboratory (HML – Charleston, SC, USA) is also greatly appreciated.

References

1. J. S. Becker, *Inorganic Mass Spectrometry: Principles and Applications*; Wiley, Chichester, 1st edn., 2007, pp. 1-6.

2. V. L. Dressler, F. G. Antes, C. M. Moreira, D. Pozebon and F. A. Duarte, *Intern. J. Mass Spectrom.*, 2011, **307**, 49-162.

3. G. Raber, N. Stock, P. Hanel, M. Murko, J. Navratilova and K.A. Francesconi, *Food Chem.*, 2012, **134**, 524-532.

4. J. Koch and D. Günther, *Appl. Spectrosc.*, 2011, **65**, 155-162.

5. J. Avivar, L. Ferrer, M. Casas and V. Cerdà, *J. Anal. At. Spectrom.*, 2012, **27**, 327-334.

6. L. L. Fialho, C. D. Pereira and J. A. Nóbrega, *Spectrochim. Acta Part B*, 2011, **66**, 389-393.

7. S. D'Ilio, N. Violante, C. Majorani and F. Petrucci, *Anal. Chim. Acta*, 2011, **698**, 6-13.

8. A. Quemet, R. Brennetot, E. Chevalier, E. Prian, A. Laridon, C. Mariet, P. Fichet, I. Laszak and F. Goutelard, *Talanta*, 2012, **99**, 207-212.

9. R. Thomas, *Spectroscopy*, 2002, **17**, 42-48.

10. D. Pick, M. Leiterer and J. W. Einax, *Microchem. J.*, 2010, **95**, 315-319.

11. G. L. Donati, R. S. Amais and J. A. Nóbrega, *J. Braz. Chem. Soc.*, 2012, **34**, 786-791.

12. S. D. Tanner, V. I. Baranov and D. R. Bandura, *Spectrochim. Acta Part B*, 2002, **57**, 1361-1452

13. R. Thomas, *Spectroscopy*, 2001, **16**, 22-27.

14. M. Colon, M. Hidalgo and M. Iglesias, *Talanta*, 2011, **85**, 1941-1947.

15. Z. Zhang, S. Chen, H. Yu, M. Sun and W. Liu, *Anal. Chim. Acta*, 2004, **513**, 417-423.

16. G. L. Donati, R. S. Amais and J. A. Nóbrega, *J. Anal. At. Spectrom.*, 2011, **26**, 1827-1832.

17. G. L. Donati, R. S. Amais and J. A. Nóbrega, *Spectroscopy*, 2012, **27**, 44-49.

18. R. S. Amais, G. L. Donati and J. A. Nóbrega, *Anal. Chim. Acta*, 2011, **706**, 223-228.

19. R. S. Amais, G. L. Donati and J. A. Nóbrega, *J. Braz. Chem. Soc.*, 2012, **23**, 797-803.

20. G. L. Donati , R. S. Amais and J. A. Nóbrega, *J. Anal. At. Spectrom.*, 2012, **27**, 1274-1279.

21. National Oceanic and Atmospheric Administration. www.srh.noaa.gov, Accessed May, 2013.

Tables

Table 1 High-resolution ICP-MS instrumental conditions.

Parameter	Value
Radio frequency applied power (kW)	1.35
Argon flow rate (L min^{-1})	
Plasma	16.0
Auxiliary	0.8
Sample	1.355
Peristaltic pump rate (rpm)	8.0
Scan type	E-Scan
Detection mode	Triple

Table 2 Mass ranges of each specie monitored.

Specie	Mass range (amu)
^{28}Si	27.975 - 27.978
$^{12}C^{16}O$	27.993 - 27.996
$^{14}N^{14}N$	28.004 - 28.007
^{32}S	31.970 - 31.974
$^{16}O^{16}O$	31.987 - 31.991
^{34}S	33.965 - 33.969
$^{16}O^{18}O$	33.991 - 33.996
^{36}Ar	35.965 - 35.969
^{36}ArH	36.973 - 36.977
^{38}Ar	37.960 - 37.965
^{39}K	38.961 - 38.966
^{38}ArH	38.968 - 38.972
^{75}As	74.916 - 74.926
$^{40}Ar^{35}Cl$	74.926 - 74.935

Table 3 Mathematically calculated and experimentally determined recoveries for $^{39}K^+$ determined by low resolution ICP-MS. Calculated values are based on Eqns. 1 and 2. Signal intensities from $^{38}ArH^+$ and $^{39}K^+$, monitored by HR-SF-ICP-MS, were summed to simulate low resolution determinations at m/z 39.

[K] (µg/L)	**Without IFS correction**		**39/$^{36}Ar^+$**		**39/$^{36}ArH^+$**		**39/$^{38}Ar^+$**	
	Calculated	Determined	Calculated	Determined	Calculated	Determined	Calculated	Determined
5	76.8	61.3	103.9	119.7	106.9	102.8	123.9	131.0
20	98.1	91.2	103.2	94.7	97.6	95.3	97.6	97.1
50	103.7	105.1	97.4	94.8	96.2	96.5	96.9	96.5

Table 4 Interfering-to-analyte signal ratios (I_I/I_A), and interfering ion and IFS species ($^{36}Ar^+$, $^{36}ArH^+$ and $^{38}Ar^+$) signal intensity variations between standard reference solutions and samples containing K.

[K](µg L^{-1})	**I_I/I_A**	**V_I (%)[a]**	**V_{36Ar+} (%)[a]**	**V_{36ArH+} (%)[a]**	**V_{38Ar+} (%)[a]**
5	7.5	-3.1	-3.2	-3.5	-5.4
20	1.9	-1.0	-1.8	0.1	0.1
50	0.8	4.6	3.6	4.2	3.8

[a] $V = \frac{(Sample\ solution\ signal - Standard\ reference\ solution\ signal)}{Standard\ reference\ solution\ signal}\ x\ 100$

Figure captions

Fig. 1 Relative HR-SF-ICP-MS signal intensities of $^{38}ArH^+$ and IFS species ($^{36}Ar^+$, $^{36}ArH^+$, $^{38}Ar^+$) while introducing K standard solution in HNO_3 1% v/v (blank, 1, 5, 20 and 50 µg L^{-1} - measurements 1, 3, 5, 7 and 9, respectively) and SRM 1643e diluted in HNO_3 1% v/v for a K final concentration of blank, 1, 5, 20 and 50 µg L^{-1} (measurements 2, 4, 6, 8 and 10, respectively).

Fig. 2 HR-SF-ICP-MS signal intensities profile of $^{40}Ar^{35}Cl^+$ compared to $^{36}Ar^+$ (A), $^{36}ArH^+$ (B) and $^{38}Ar^+$ (C) IFS species while introducing As standard solution in HCl 1% v/v (blank, 1, 5 and 20 µg L^{-1} - measurements 1, 3, 5 and 7, respectively) and SRM 1643e diluted in HCl 1% v/v for a As final concentration of blank, 1, 5 and 20 (measurements 2, 4, 6 and 8, respectively).

Fig. 3 Sum of $^{75}As^+$ and $^{40}As^{35}Cl^+$ signal intensities obtained for As standard solution in HCl 1% v/v (1, 5, 20 and 50 µg L^{-1}) and for SRM 1643e diluted in HCl 1% v/v for a As final concentration of 1, 5, 20 and 50 µg L^{-1} (A) compared to the results obtained with IFS correction using $^{36}Ar^+$ (B), $^{36}ArH^+$ (C) and $^{38}Ar^+$ (D) probes.

Fig. 4 Profile of the sum of interfering ions ($^{14}N_2^+$ + $^{12}C^{16}O^+$) signal intensities obtained in HR-SF-ICP-MS and $^{36}Ar^+$ (A), $^{36}ArH^+$ (B) and $^{38}Ar^+$ (C) IFS species while introducing Si standard solution in HNO_3 1% v/v (blank, 20, 50, 100, 200 and 500 µg L^{-1} - measurements 1, 3, 5, 7, 9 and 11 respectively) and tap water diluted in HNO_3 1% v/v (0.1:10) containing Si final

concentration of blank, 20, 50, 100, 200 and 500 µg L^{-1} (measurements 2, 4, 6, 8, 10 and 12 respectively).

Fig. 5 Profile of $^{16}O_2^+$ interfering ion signal intensities obtained in HR-SF-ICP-MS and $^{36}Ar^+$ (A), $^{36}ArH^+$ (B) and $^{38}Ar^+$ (C) IFS species while introducing S standard solution in HNO_3 1% v/v (0.5, 1, 5, 10 and 50 mg L^{-1} - measurements 1, 3, 5, 7 and 9, respectively) and tap water diluted in HNO_3 1% v/v (0.1:10) containing S final concentration of 0.5, 1, 5, 10 and 50 mg L^{-1} (measurements 2, 4, 6, 8 and 10, respectively).

Figures

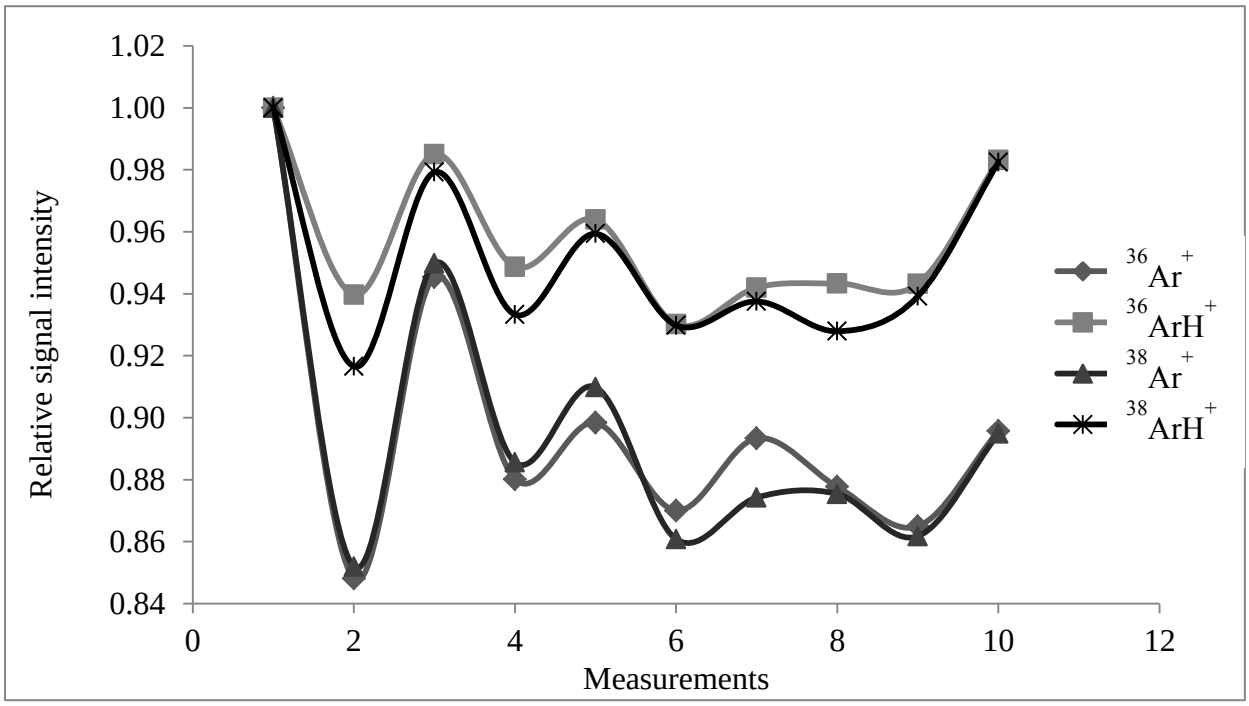

Fig. 1 Relative HR-SF-ICP-MS signal intensities of $^{38}ArH^{+}$ and IFS species ($^{36}Ar^{+}$, $^{36}ArH^{+}$, $^{38}Ar^{+}$) while introducing K standard solution in HNO_3 1% v/v (blank, 1, 5, 20 and 50 µg L^{-1} - measurements 1, 3, 5, 7 and 9, respectively) and SRM 1643e diluted in HNO_3 1% v/v for a K final concentration of blank, 1, 5, 20 and 50 µg L^{-1} (measurements 2, 4, 6, 8 and 10, respectively).

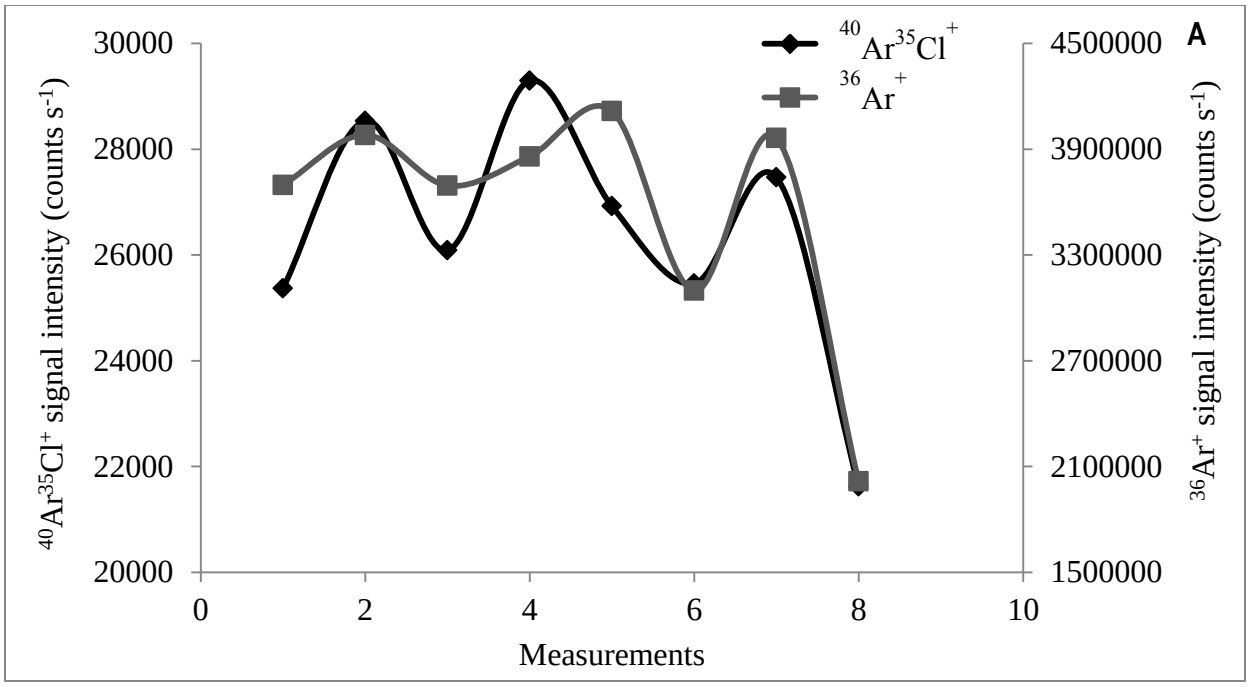

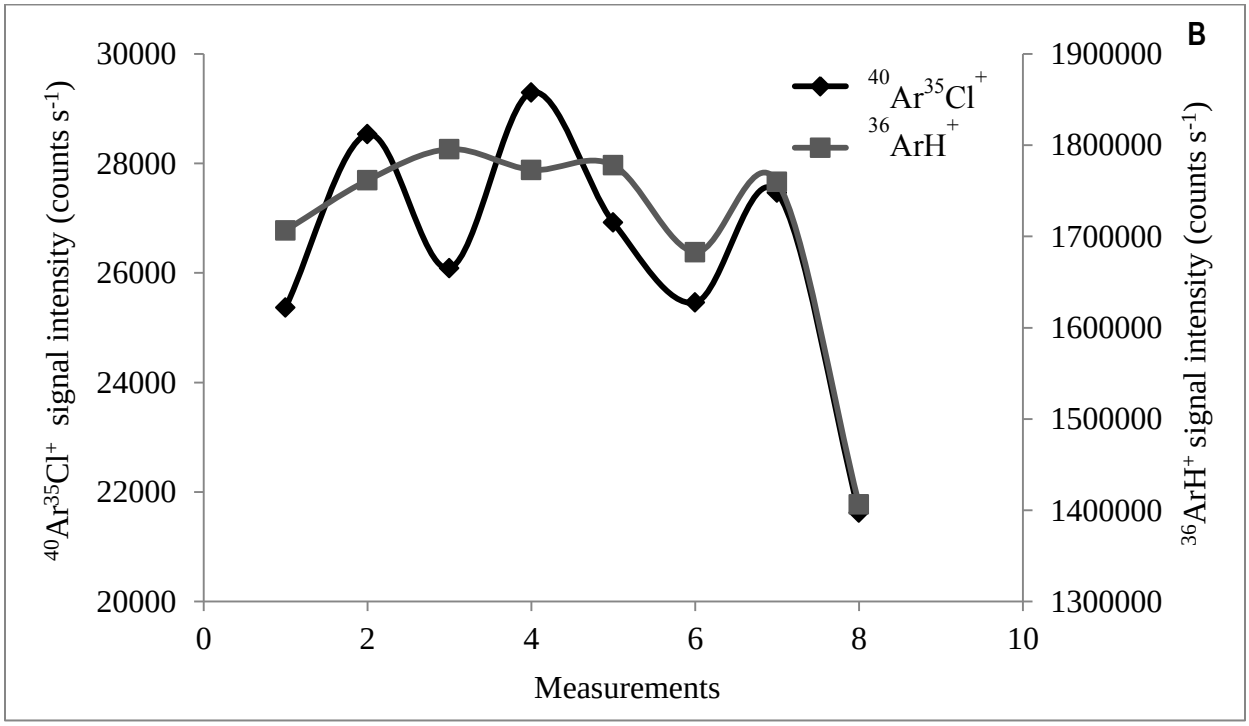

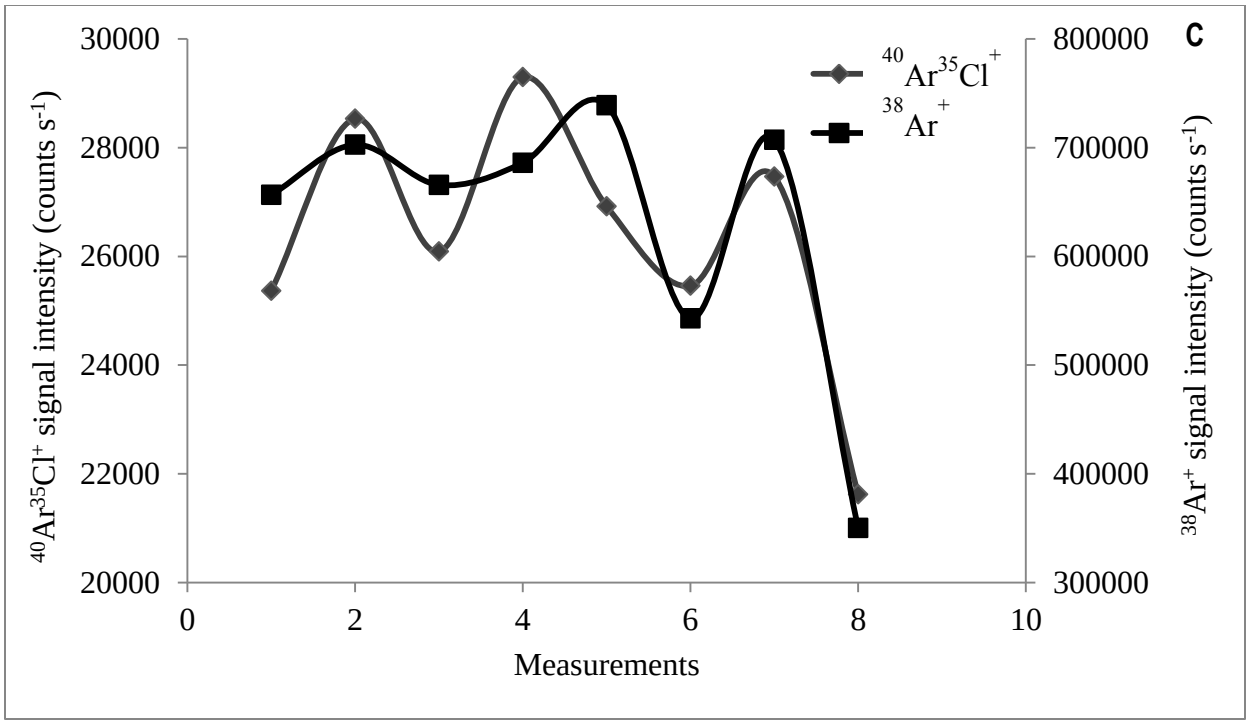

Fig. 2 HR-SF-ICP-MS signal intensities profile of $^{40}Ar^{35}Cl^{+}$ compared to $^{36}Ar^{+}$ (A), $^{36}ArH^{+}$ (B) and $^{38}Ar^{+}$ (C) IFS species while introducing As standard solution in HCl 1% v/v (blank, 1, 5 and 20 µg L^{-1} - measurements 1, 3, 5 and 7, respectively) and SRM 1643e diluted in HCl 1% v/v for a As final concentration of blank, 1, 5 and 20 µg L-1 (measurements 2, 4, 6, and 8, respectively).

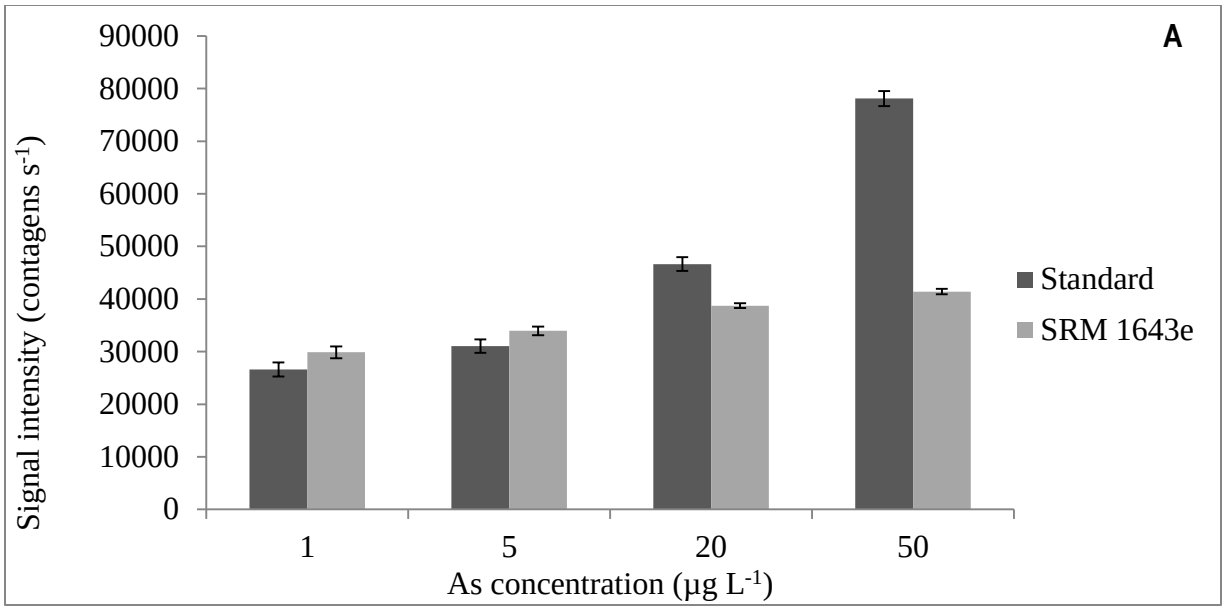

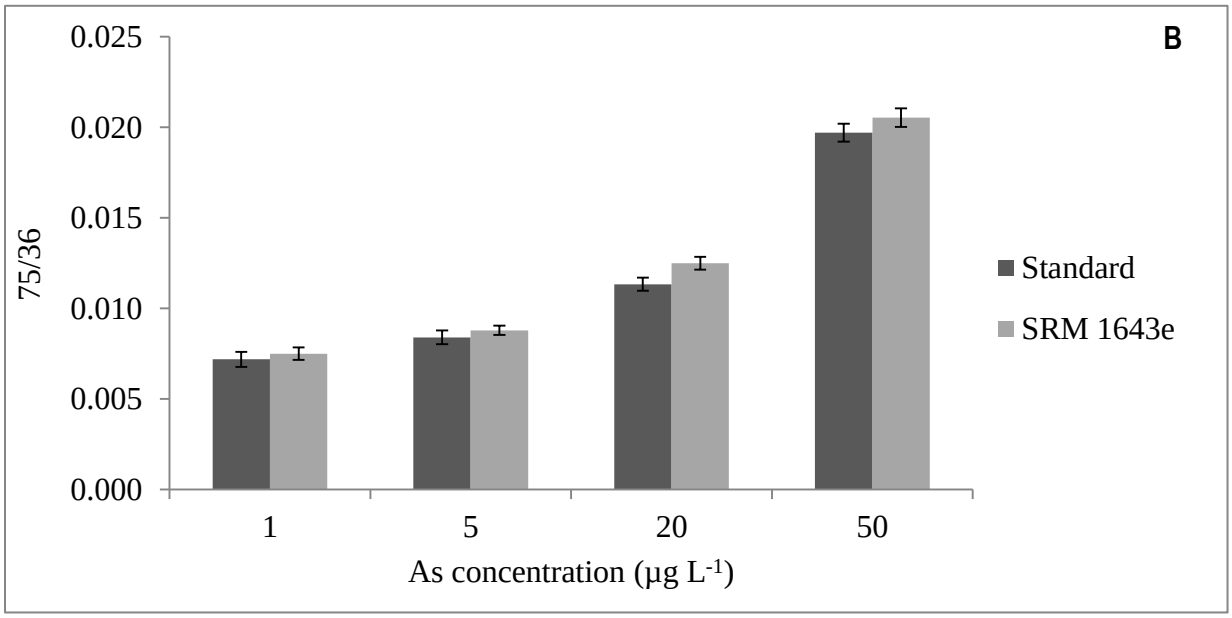

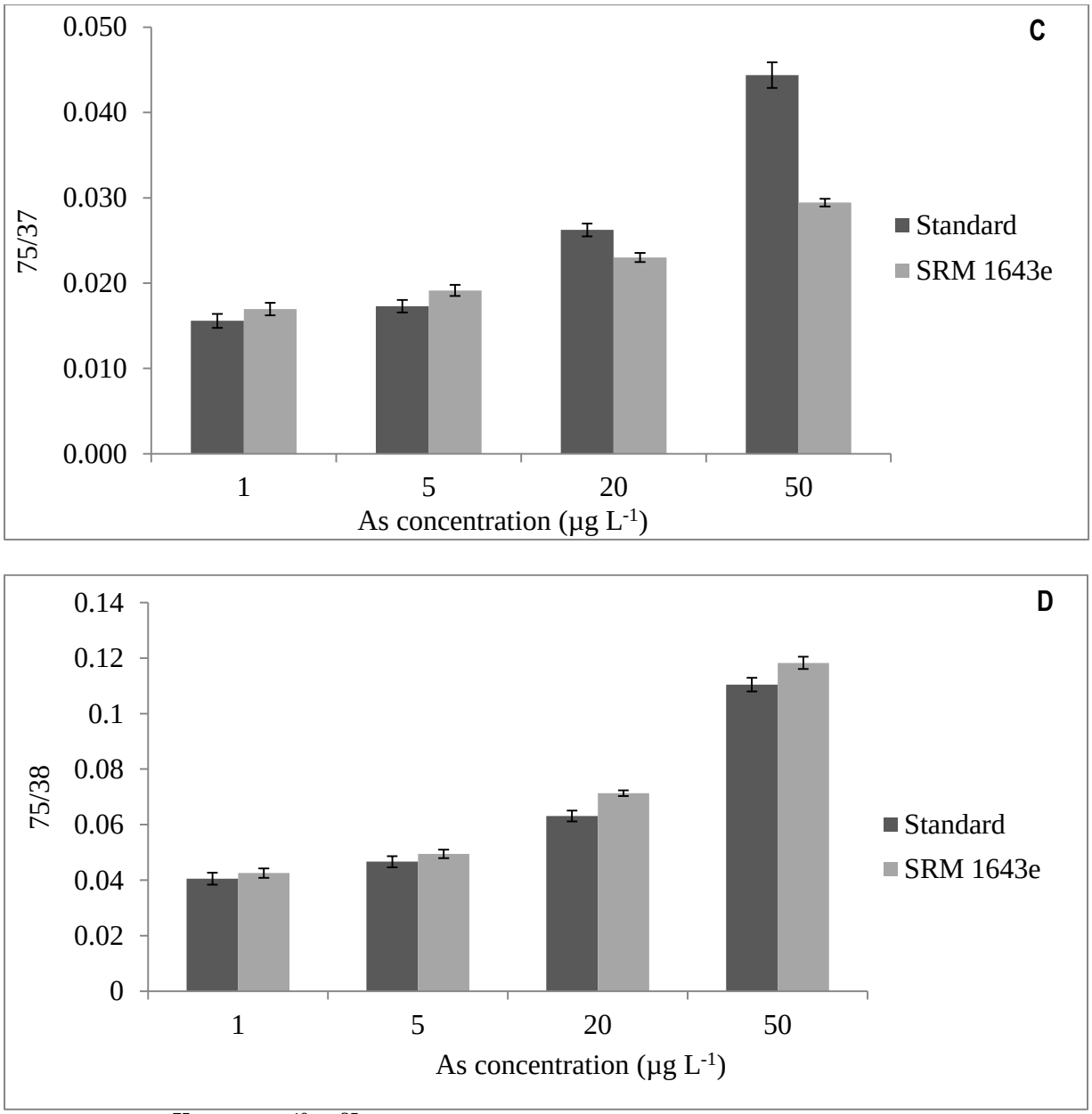

Fig. 3 Sum of $^{75}As^{+}$ and $^{40}As^{35}Cl^{+}$ signal intensities obtained for As standard solution in HCl 1% v/v (1, 5, 20 and 50 µg L^{-1}) and for SRM 1643e diluted in HCl 1% v/v for a As final concentration of 1, 5, 20 and 50 µg L^{-1} (A) compared to the results obtained with IFS correction using $^{36}Ar^{+}$ (B), $^{36}ArH^{+}$ (C) and $^{38}Ar^{+}$ (D) probes.

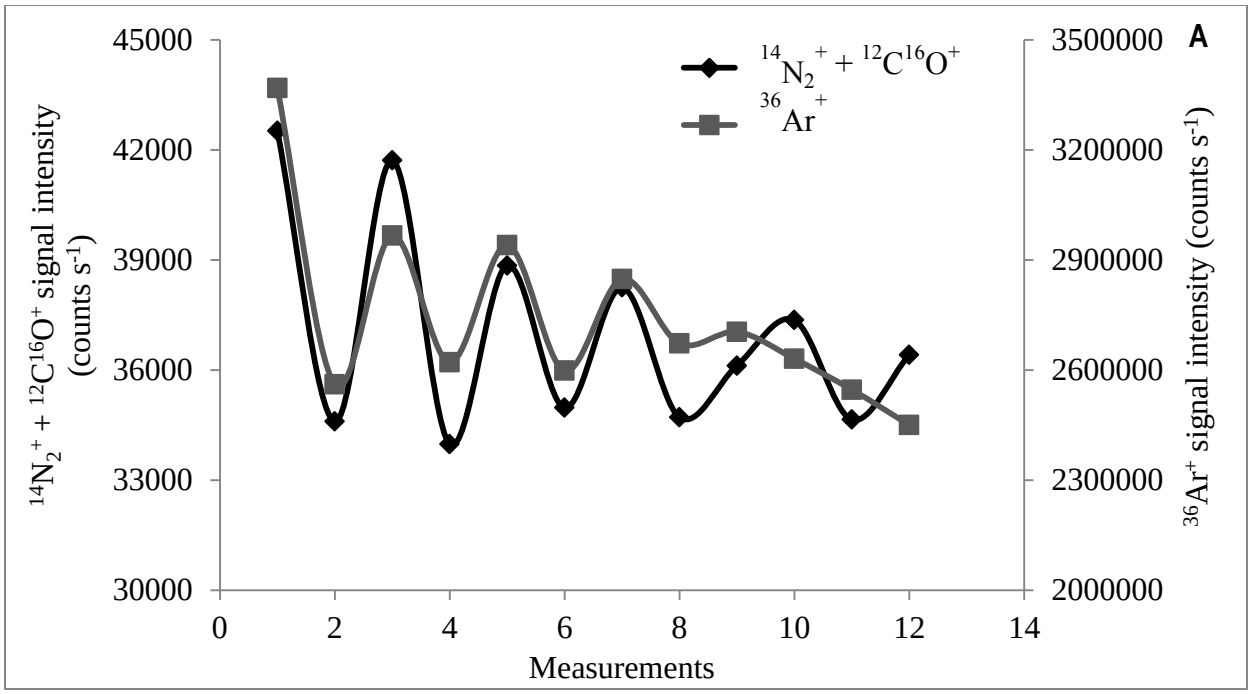

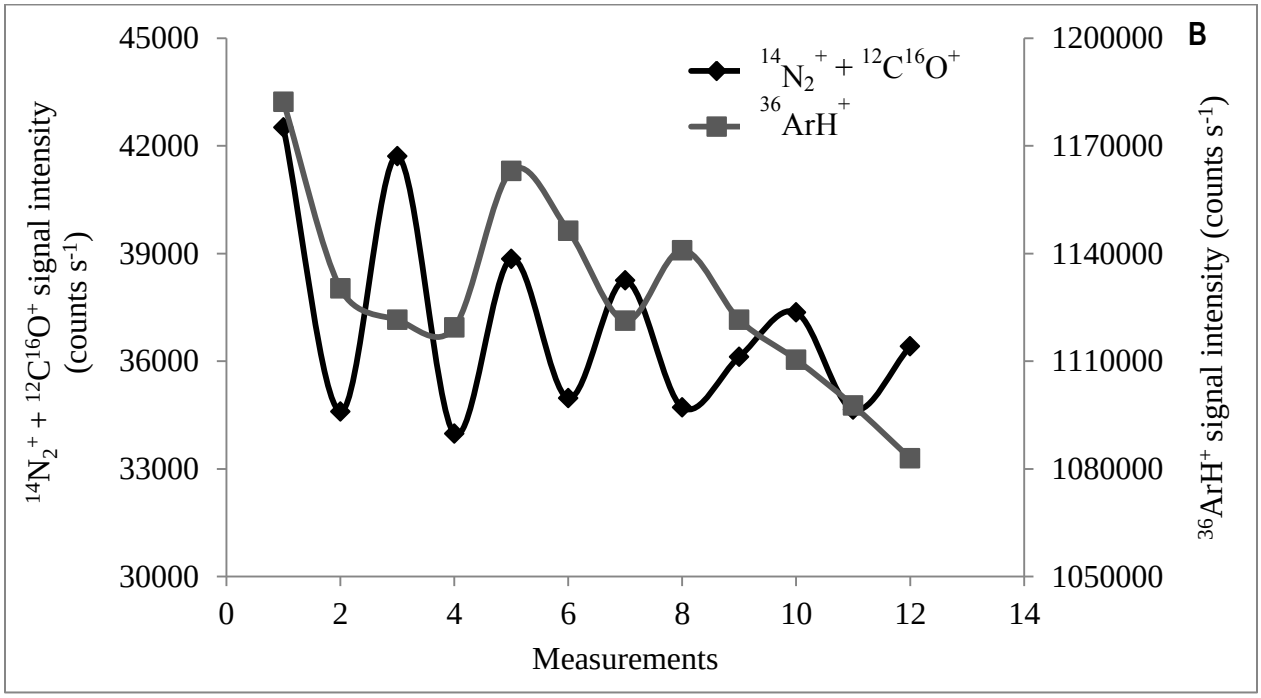

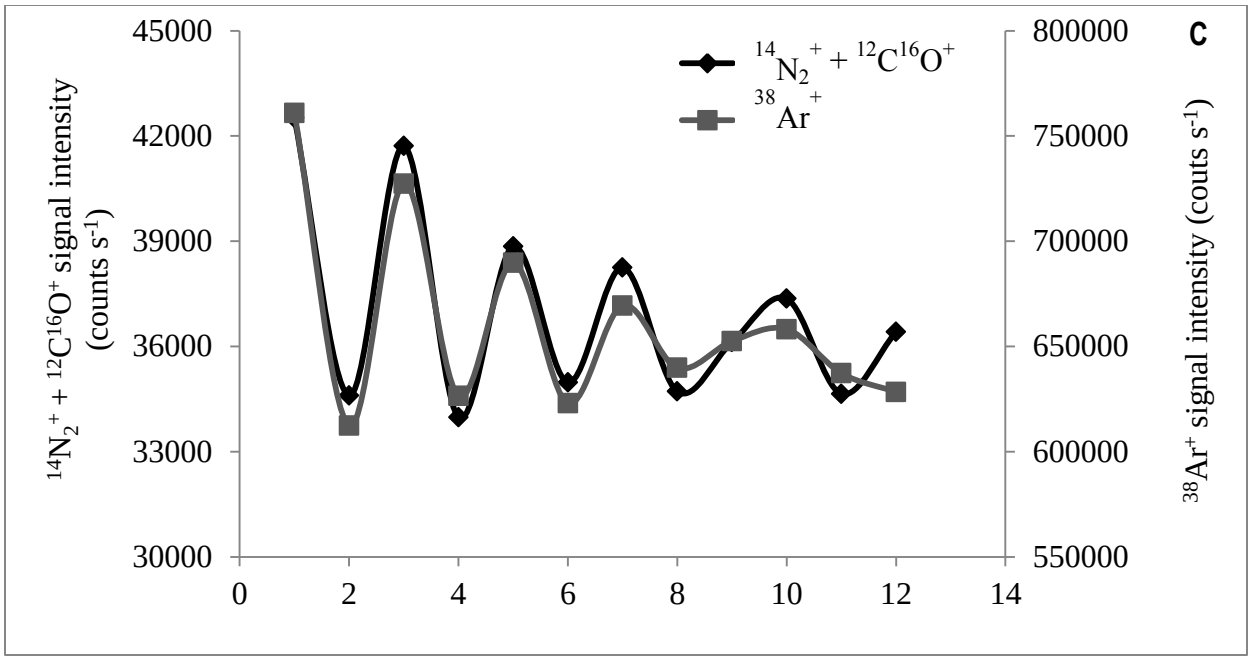

Fig. 4 Profile of the sum of interfering ions ($^{14}N_2^+ + {}^{12}C^{16}O^+$) signal intensities obtained in HR-SF-ICP-MS and $^{36}Ar^+$ (A), $^{36}ArH^+$ (B) and $^{38}Ar^+$ (C) IFS species while introducing Si standard solution in HNO_3 1% v/v (blank, 20, 50, 100, 200 and 500 µg L^{-1} - measurements 1, 3, 5, 7, 9 and 11 respectively) and tap water diluted in HNO_3 1% v/v (0.1:10) containing Si final concentration of blank, 20, 50, 100, 200 and 500 µg L^{-1} (measurements 2, 4, 6, 8, 10 and 12 respectively).

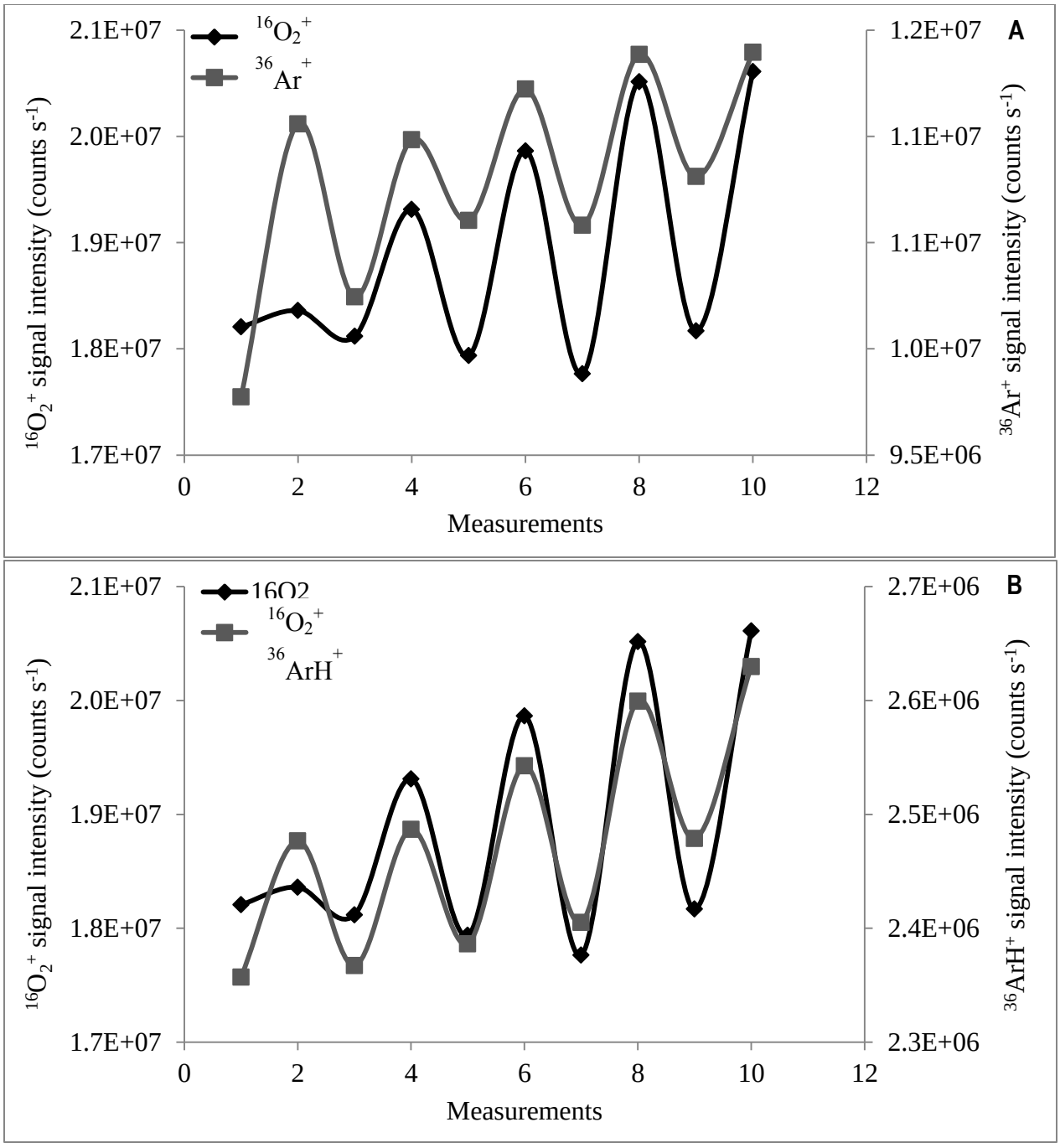

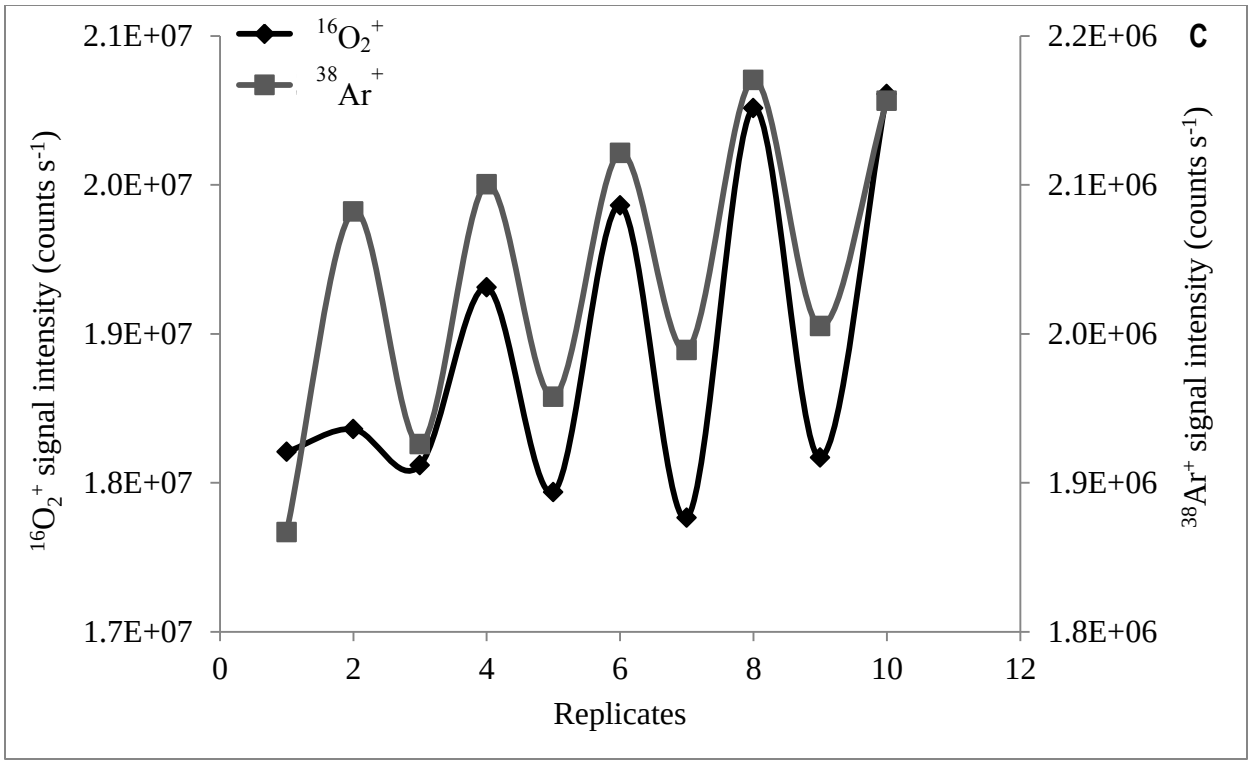

Fig. 5 Profile of $^{16}O_2^+$ interfering ion signal intensities obtained in HR-SF-ICP-MS and $^{36}Ar^+$ (A), $^{36}ArH^+$ (B) and $^{38}Ar^+$ (C) IFS species while introducing S standard solution in HNO_3 1% v/v (0.5, 1, 5, 10 and 50 mg L^{-1} - measurements 1, 3, 5, 7 and 9, respectively) and tap water diluted in HNO_3 1% v/v (0.1:10) containing S final concentration of 0.5, 1, 5, 10 and 50 mg L^{-1} (measurements 2, 4, 6, 8 and 10, respectively).